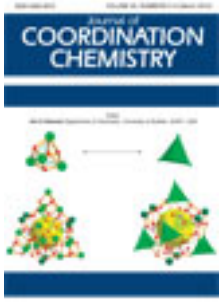


Journal of Coordination Chemistry
Publication details, including instructions for authors and subscription information:
http://www.tandfonline.com/loi/gcoo20

# Hydrothermal synthesis, structure, and properties of two new nanosized $Ln_{26}$ (Ln=Ho, Er) clusters

Lei Chen [a], Lian Huang [a], Congling Wang [a], Jie Fu [a], Deng Zhang [a], Dunru Zhu [a] & Yan Xu [a b]

[a] College of Chemistry and Chemical Engineering, State Key Laboratory of Materials-Oriented Chemical Engineering, Nanjing University of Technology, Nanjing 210009, P.R. China

[b] Coordination Chemistry Institute, State Key Laboratory of Coordination Chemistry, Nanjing University, Nanjing 210093, P.R. China

Published online: 27 Feb 2012.

To cite this article: Lei Chen, Lian Huang, Congling Wang, Jie Fu, Deng Zhang, Dunru Zhu & Yan Xu (2012) Hydrothermal synthesis, structure, and properties of two new nanosized $Ln_{26}$ (Ln=Ho, Er) clusters, Journal of Coordination Chemistry, 65:6, 958-968, DOI: 10.1080/00958972.2012.664768

To link to this article: http://dx.doi.org/10.1080/00958972.2012.664768

*Journal of Coordination Chemistry*
Vol. 65, No. 6, 20 March 2012, 958–968



# Hydrothermal synthesis, structure, and properties of two new nanosized $Ln_{26}$ (Ln = Ho, Er) clusters

LEI CHEN†, LIAN HUANG†, CONGLING WANG†, JIE FU†, DENG ZHANG†, DUNRU ZHU† and YAN XU*†‡

†College of Chemistry and Chemical Engineering, State Key Laboratory of Materials-Oriented Chemical Engineering, Nanjing University of Technology, Nanjing 210009, P.R. China
‡Coordination Chemistry Institute, State Key Laboratory of Coordination Chemistry, Nanjing University, Nanjing 210093, P.R. China

(*Received 16 November 2011; in final form 9 January 2012*)

Two new compounds, $[Ho_{26}(IN)_{28}(CH_3COO)_4(CO_3)_{10}(OH)_{26}(H_2O)_{18}]\cdot 20H_2O$ (**1**) (HIN = isonicotinic acid) and $[Er_{26}(IN)_{29}(CH_3COO)_3(CO_3)_{10}(OH)_{26}(H_2O)_{19}]\cdot 26H_2O$ (**2**), employing the building unit of $CO_3@Ln_{26}$ have been synthesized hydrothermally. Compound **1** crystallizes in the triclinic space group $P\bar{1}$ with $a = 21.043(4)$ Å, $b = 21.128(5)$ Å, $c = 35.140(8)$ Å, $\alpha = 85.838(3)^\circ$, $\beta = 74.909(3)^\circ$, $\gamma = 85.414(3)^\circ$, $V = 15{,}014(6)$ Å$^3$, $Z = 2$; **2** crystallizes in triclinic $P\bar{1}$ with $a = 20.9968(15)$ Å, $b = 21.1260(15)$ Å, $c = 35.125(3)$ Å, $\alpha = 85.9530(10)^\circ$, $\beta = 74.7590(10)^\circ$, $\gamma = 85.5020(10)^\circ$, $V = 14{,}966.3(18)$ Å$^3$, $Z = 2$. In the structures of both compounds, the isonicotinate (IN) is the main ligand while $CH_3COO^-$ functions as the second ligand to stabilize the $Ln_{26}$ cluster; $CO_3^{2-}$ plays a very important role in the formation of the spherical $Ln_{26}$ cluster. The two compounds are isostructural and have been characterized by single-crystal X-ray diffraction, IR absorption spectroscopy, thermogravimetric analysis, ultraviolet excitation, and emission spectrum.

*Keywords*: Nanosized Ln–O cluster; Hydrothermal synthesis; Crystal structure



## 1. Introduction

Nanosized high-nuclearity metal complexes have gained intense attention [1, 2] from their aesthetically pleasing structures and useful properties such as magnetism, optics, electronics, and catalysis [3–7]. A large amount of transition metal clusters of high-nuclearity have been documented, such as molybdenum [8–11], silver [12, 13], manganese [14], nickel [15], and copper clusters [16]. However, the analogous construction of lanthanides is still in its infancy as lanthanides have essential characteristics including high, variable coordination numbers, and small energy difference in the various coordination geometries [17–21]. Clusters like $[Ln_7]$, $[Ln_8]$,

*Corresponding author. Email: yanxu@njut.edu.cn


ISSN 0095-8972 print/ISSN 1029-0389 online 
http://dx.doi.org/10.1080/00958972.2012.664768

$[Ln_{10}]$, $[Ln_{12}]$, $[Ln_{14}]$, $[Ln_{15}]$, $[Ln_{20}]$, $[Ln_{26}]$, $[Ln_{34}]$, and $[Er_{60}]$ [22–35] are the reported lanthanide clusters thus far, either pure lanthanide-based clusters or mixed 3d–4f heterometallic systems. As a general rule, they were synthesized utilizing the strategy of controlling the hydrolysis of lanthanide clusters in the presence of supporting ligands such as $CN^-$, carbonyl, amino acids, and pyridinecarboxylate. Based on this strategy, our research group had synthesized several $[Ln_{26}]$ clusters, including two 3-D 3d–4f coordination polymers constructed from nanosized cage-shaped hydroxo $Ln_{26}$ clusters and Zn centers [34] and some other 4d–4f compounds. In this work, we prepare two new $Ln_{26}$ high-nuclearity clusters formulated as $[Ho_{26}(IN)_{28}(CH_3COO)_4(CO_3)_{10}(OH)_{26}(H_2O)_{18}]\cdot 20H_2O$ (**1**; IN = isonicotinate) and $[Er_{26}(IN)_{29}(CH_3COO)_3(CO_3)_{10}(OH)_{26}(H_2O)_{19}]\cdot 26H_2O$ (**2**). In the structures of both compounds, nine $CO_3^{2-}$ groups bond 26 $Ln^{3+}$ to form a central closed $Ln_{26}$ cage, which surrounds a remaining free $CO_3^{2-}$. Isonicotinic acid (HIN) as the supporting ligand and $CH_3COO^-$ as a second ligand stabilize the $Ln_{26}$ cluster cage.



## 2. Experimental

### 2.1. *Materials and methods*

All reagents were of commercial origin and used without purification. C, H, and N elemental analyses were performed on a Perkin-Elmer 2400 CHN elemental analyzer. Infrared (IR) spectra of the two compounds were obtained as pressed KBr pellets on a Nicolet Impact 410 FTIR spectrometer. Thermogravimetric (TG) analysis was carried out in flowing $N_2$ atmosphere from 35°C to 900°C with a heating rate of 10°C $min^{-1}$ with a Diamond thermogravimetric analyzer.

### 2.2. *Syntheses of the complexes*

**2.2.1. $[Ho_{26}(IN)_{28}(CH_3COO)_4(CO_3)_{10}(OH)_{26}(H_2O)_{18}]\cdot 20H_2O$.** A mixture of $Ho_2O_3$ (0.2077 g, 0.55 mmol), $Mn(OAc)_2\cdot 4H_2O$ (0.0353 g, 0.14 mmol), HIN (0.2460 g, 2.00 mmol), HCOOH (88%, 0.0184 g, 0.35 mmol), and $H_2O$ (8.00 mL) was placed in a 25 mL Teflon-lined autoclave. The pH of the solution was adjusted to 2.0 with HCl (36%) and then the solution was sealed after stirring for 12 h and kept at 170°C for 7 days; light-yellow block crystals of **1** were obtained (0.1884 g, yield of 41% based on Ho). Elemental Anal. Calcd (%): C, 23.05; H, 2.35; N, 4.05; Found (%): C, 22.94; H, 2.26; N, 4.13.

**2.2.2. $[Er_{26}(IN)_{29}(CH_3COO)_3(CO_3)_{10}(OH)_{26}(H_2O)_{19}]\cdot 26H_2O$.** The synthesis procedure of **2** is similar to that of **1** except that $Ho_2O_3$ was replaced by $Er_2O_3$ (0.2103 g, 0.55 mmol); light-pink block crystals of **2** were prepared (0.1635 g, yield of 39% based on Er). Elemental Anal. Calcd (%): C, 22.99; H, 2.43; N, 4.09; Found (%): C, 22.93; H, 2.38; N, 4.16.

Table 1. Crystal data and structure refinement for **1** and **2**.

| Compound | **1** | **2** |
|---|---|---|
| Empirical formula | $Ho_{26}N_{28}C_{186}O_{158}H_{226}$ | $Er_{26}N_{29}C_{190}O_{165}H_{241}$ |
| Formula weight | 9670.13 | 9919.86 |
| Temperature (K) | 296(2) | 296(2) |
| Wavelength (Å) | 0.71073 | 0.71073 |
| Crystal system | Triclinic | Triclinic |
| Space group | $P\bar{1}$ | $P\bar{1}$ |
| Unit cell dimensions (Å, °) | | |
| $a$ | 21.043(4) | 20.9968(15) |
| $b$ | 21.128(5) | 21.1260(15) |
| $c$ | 35.140(8) | 35.125(3) |
| $\alpha$ | 85.838(3) | 85.9530(10) |
| $\beta$ | 74.909(3) | 74.7590(10) |
| $\gamma$ | 85.414(3) | 85.5020(10) |
| Volume (Å$^3$), $Z$ | 15014(6), 2 | 14966.3(18), 2 |
| Calculated density (g cm$^{-3}$) | 2.139 | 2.201 |
| Absorption coefficient (mm$^{-1}$) | 6.860 | 7.303 |
| $F$(000) | 9088 | 9340 |
| Crystal size (mm$^3$) | $0.15 \times 0.13 \times 0.12$ | $0.13 \times 0.11 \times 0.10$ |
| Limiting indices | $-24 \le h \le 25$;<br>$-24 \le k \le 25$;<br>$-41 \le l \le 41$ | $-25 \le h \le 23$;<br>$-25 \le k \le 23$;<br>$-42 \le l \le 42$ |
| Reflections collected | 104,465 | 109,807 |
| Independent reflection | 51,863 [$R$(int) = 0.0536] | 54,639 [$R$(int) = 0.0461] |
| Max. and min. transmission | 0.4932 and 0.4260 | 0.5288 and 0.4503 |
| Refinement method | Full-matrix-block least-squares on $F^2$ | Full-matrix-block least-squares on $F^2$ |
| Data/parameters | 51,863/1727 | 54,639/1772 |
| Goodness-of-fit on $F^2$ | 1.006 | 1.046 |
| Final $R$ indices [$I > 2\sigma(I)$] | $R_1 = 0.0778$, $wR_2 = 0.2140$ | $R_1 = 0.0541$, $wR_2 = 0.1494$ |
| $R$ indices (all data) | $R_1 = 0.1148$, $wR_2 = 0.2268$ | $R_1 = 0.0802$, $wR_2 = 0.1699$ |

### 2.3. *X-ray crystallography*

Single crystals of the compounds were glued to a thin glass fiber with epoxy glue in air for data collection; diffraction data were performed on a Bruker Apex II CCD with Mo-K$\alpha$ radiation ($\lambda = 0.71073$ Å) at 296 K using $\omega$–$2\theta$ scan method. An empirical absorption correction was applied. The structures were solved by direct methods and refined by full-matrix least-squares on $F^2$ using the SHELX-97 program package [36]. Because there are about 400 crystallographic independent non-hydrogen atoms, the metals were refined anisotropically while the O, C, and N of ligands for both compounds were refined isotropically. Hydrogen atoms of the organic moieties were placed in calculated positions, assigned isotropic displacement parameters, and allowed to ride on their parent atoms. However, hydrogen atoms for water molecule and $OH^-$ are not located. Crystallographic data and relevant information are presented in table 1.

## 3. Results and discussion

### 3.1. *Crystal structure*

The experimental and simulated XRD patterns of **1** and **2** are shown in figure S1a and S1b. The experimental peak positions of **1** and **2** are in agreement with the simulated

XRD pattern, indicating phase purity of both compounds. Single-crystal X-ray diffraction demonstrates that **1** and **2** crystallize in the low-symmetry triclinic space group $P\bar{1}$ and are isostructural. Thus, **1** is the representative of the two compounds.

Single-crystal X-ray diffraction analysis shows that **1** consists of nanosized $[Ho_{26}(IN)_{28}(CH_3COO)_4(CO_3)_9(OH)_{26}(H_2O)_{18}]^{2+}$, $CO_3^{2-}$, and lattice water molecule. As shown in figure 1, nanosized cluster core of 26 Ho are encapsulated by a coordination sphere formed by 28 isonicotinic and 4 acetate ligands as well as 18 coordination water molecules. Nine $CO_3^{2-}$ are inserted into the cluster core backbone by Ho–O coordination bonds to reinforce the huge cluster rather than $NO_3^-$ in the reported $Dy_{26}$ cluster [17]. Besides the nine-coordinated $CO_3^{2-}$, there is a free $CO_3^{2-}$ which is encapsulated in the $Ho_{26}$ backbone. The unexpected free carbonate is probably the byproduct of ligand decomposition [16]. A better way of appreciating the regular core structure is to divide the 26 Ho units into five cubane-like $[Ho_4(\mu_3\text{-}OH)_4]^{8+}$ building units and six additional Ho (Ho3, Ho6, Ho14, Ho17, Ho19, Ho24) (figure 2). Each of the $[Ho_4(\mu_3\text{-}OH)_4]^{8+}$ units consists of four Ho's sharing four $\mu_3$-OH with Ho–O distances of 2.2587(118)–2.4623(133) Å [36–43]. Among the 20 Ho ions of the $\{Ho_4\}$ units, there are two kinds of coordination modes; Ho26 is seven-coordinate in a face-centered trigonal prism, markedly different from the reported $Ln_{26}$ clusters that are eight-coordinate, dodecahedral. Among the six additional Ho ions, there are still two kinds of Ho. Ho3 and Ho19 are nine-coordinate while the remaining are eight-coordinate. The six additional Ho's connect the five $\{Ho_4\}$ units through the nine $CO_3^{2-}$ which employ the same connecting mode with five adjacent Ho's (scheme 1, I). The ligands including $IN^-$, $CH_3COO^-$, $CO_3^{2-}$, triply bridging hydroxo, and coordinated water molecule accomplish the coordination of Ho, with $IN^-$ employing three different models (scheme 1, IV–VI) and $CH_3COO^-$ adopting two models (scheme 1, II and III).

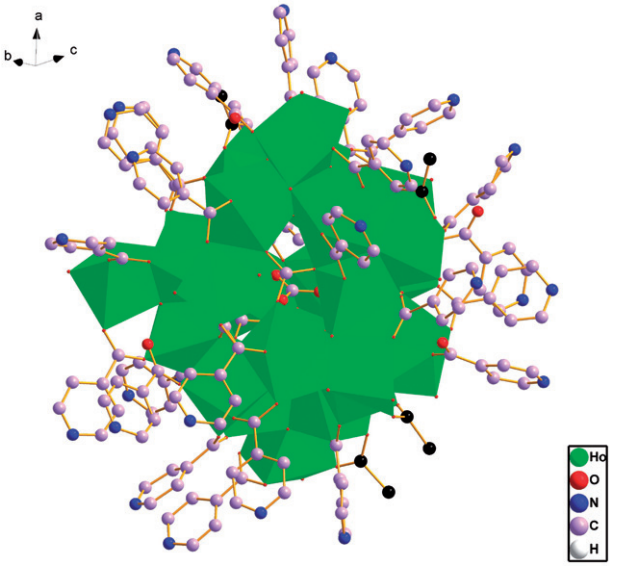


Figure 1. Crystal structure of $Ho_{26}$ complex. For clarity, hydrogen atoms and water molecule are omitted and the carbons in $CH_3COO^-$ are black.

Compared with $Zn_{1.5}Dy_{26}(IN)_{25}(CH_3COO)_8(CO_3)_{11}(OH)_{26}(H_2O)_{29}$, only four acetates coordinate to one nanosized $CO_3@Ho_{26}$ cluster; $Mn^{2+}$ are not included in **1**. The steric hindrance of **1** is little reduced in comparison to $Er_{26}I(\mu_3\text{-}OH)_{20}(\mu_3\text{-}O)_6(NO_3)_9(IN)_{33}(OH)_3(H_2O)_{33}$ [38]. As shown in figure 3, four $CO_3@Ho_{26}$ clusters link by using N···Ow (water) hydrogen bonds to form a building unit of $[CO_3@Ho_{26}]_4$, with N···O distances varying from 2.62(3) to 2.89(3) Å. Adjacent $[CO_3@Ho_{26}]_4$ units are further connected by hydrogen bonds to generate a

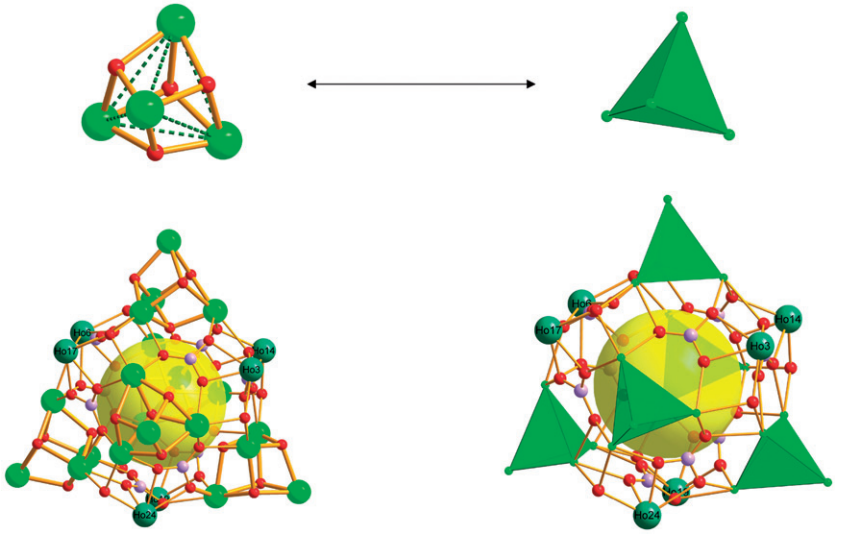

Figure 2. Illustration of the assembly of $Ho_{26}$ unit. The big yellow ball in the center of the unit represents the $CO_3^{2-}$.

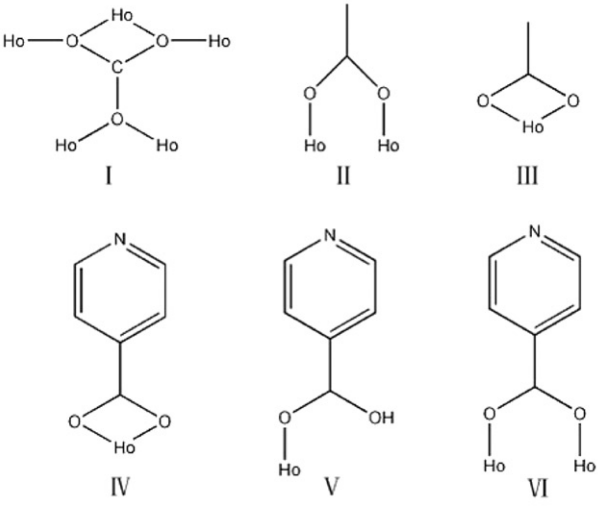


Scheme 1. Coordination modes of $CO_3^{2-}$, $CH_3COO^-$, and $IN^-$.

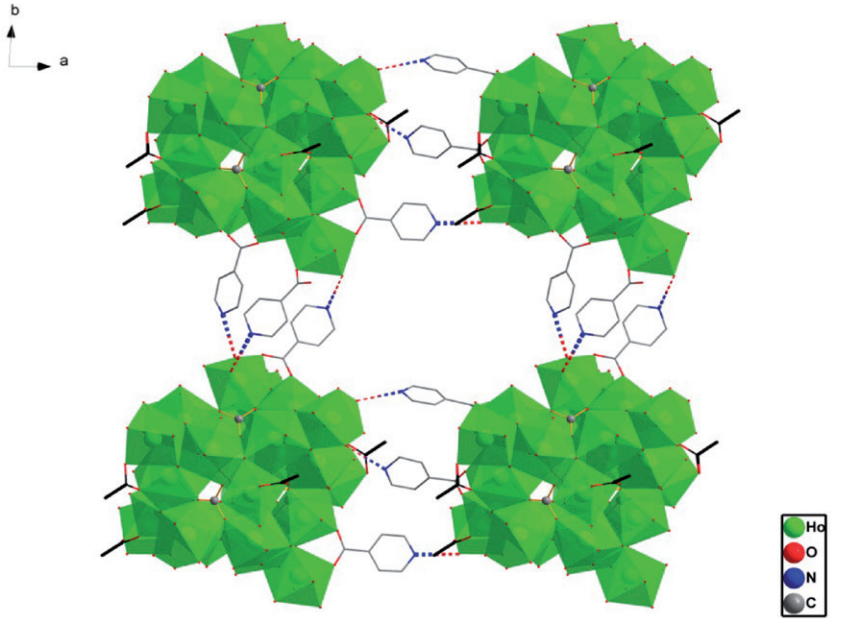


Figure 3. The $[CO_3@Ho_{26}]_4$ building unit linked by hydrogen bonding interactions N···Ow(water).

$[CO_3@Ho_{26}]_{4n}$ layer along the *c* axis, as shown in figure 4. The $[CO_3@Ho_{26}]_{4n}$ layer also involves hydrogen bonding with neighboring layers to make a 3-D supermolecule (figure 5), unlike other lanthanide supermolecules with isonicotinate connected by $\pi$–$\pi$ interactions [41]. As special free spaces are arranged in 3-D supermolecular framework of **1**, an interesting $(H_2O)_{15}$ chain (figure 6) is observed in **1**. This water cluster is reminiscent of other hydrate-supramolecular aggregates [39, 40]. Furthermore, there are other intermolecular hydrogen bonds between the lattice water molecules in addition to the water cluster and between lattice water molecules and nitrogen from $IN^-$. These hydrogen bonds play critical roles in stabilizing the crystal structure.

Replacing $Ho_2O_3$ by $Er_2O_3$, we got **2** (figure 7), whose structure is quite similar to that of **1**. The very modest difference is all Er ions in the $[Er_4(\mu_3\text{-}OH)_4]^{8+}$ building units are eight-coordinate in **2**, while Ho26 is seven-coordinate in **1**. As the cluster core of **2** is stabilized by 29 $IN^-$, 3 $CH_3COO^-$, and 18 coordination water molecules, a little different from **1**, the total ligands of **1** and **2** are the same. There is one more $IN^-$ in **2**, which leads to the different coordination environments of the Ln between **1** and **2**, and the water clusters within **2** are slightly different than **1** (figure 8), though they are of the same 3-D open framework.

### 3.2. *IR spectrum*

As shown in figure S2, the broad band at 3402 $cm^{-1}$ for **1** and 3408 $cm^{-1}$ for **2** can be ascribed to hydroxyl stretching vibration from the ligands and water molecule. The four strong peaks at 1595–1102 $cm^{-1}$ for **1** and 1670–1415 $cm^{-1}$ for **2** attest to the existence of phenyl in $IN^-$. Bands at 817–608 $cm^{-1}$ (**1**) and 861–696 $cm^{-1}$ (**2**) are associated with $\nu$(Ho–O) (**1**) and $\nu$(Er–O) (**2**).

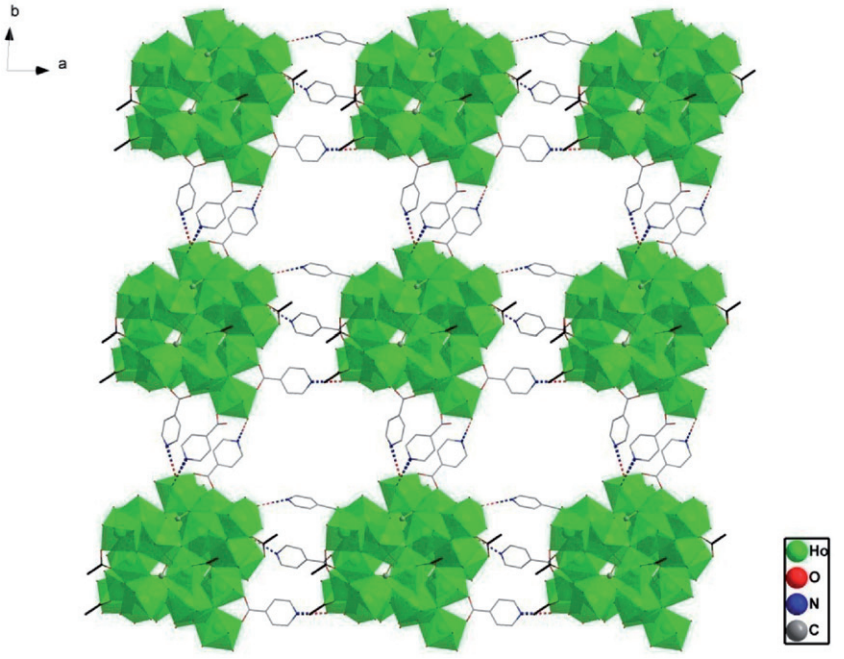


Figure 4. The $[CO_3@Ho_{26}]_{4n}$ layer along the $c$ axis.

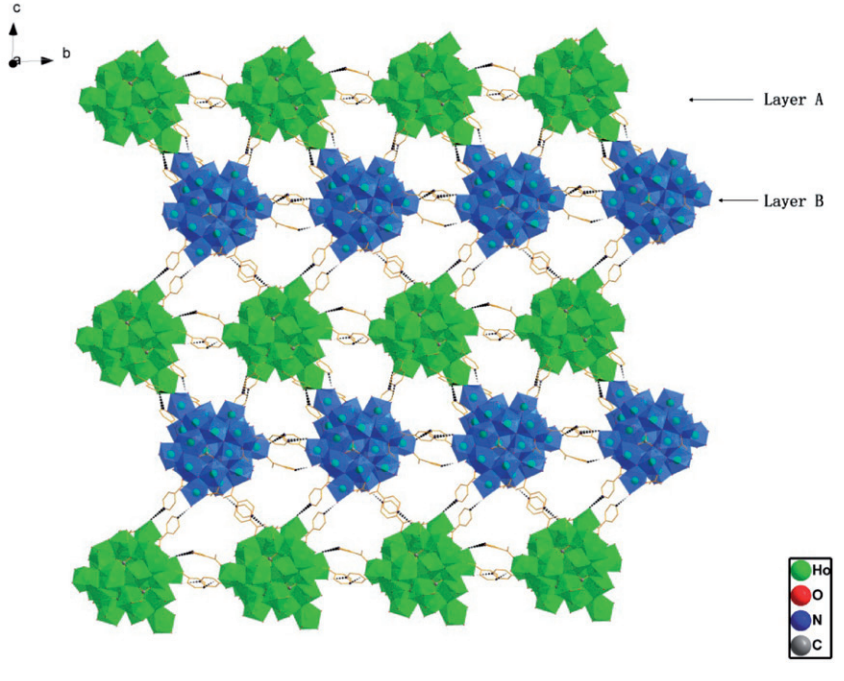


Figure 5. The neighboring $[CO_3@Ho_{26}]_{4n}$ layer in the 3-D supermolecular framework linked by hydrogen bonding.

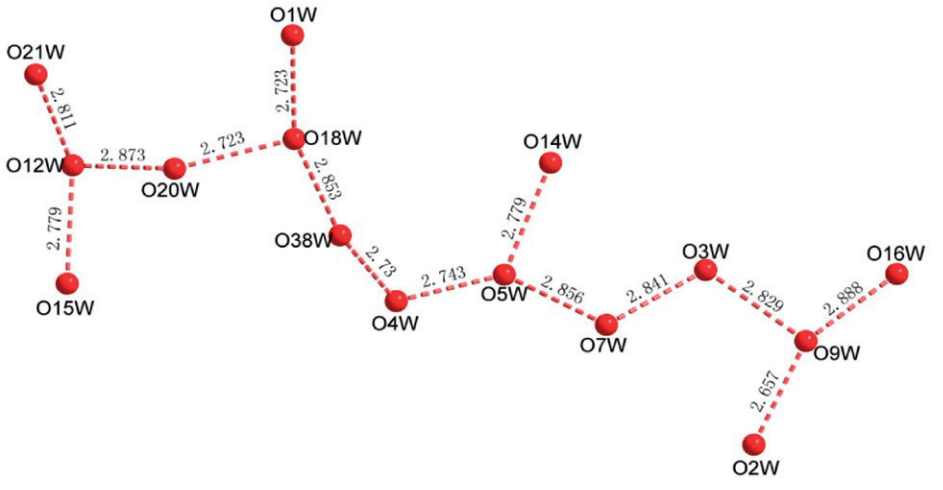


Figure 6. The interesting $(H_2O)_{15}$ water cluster in **1**.

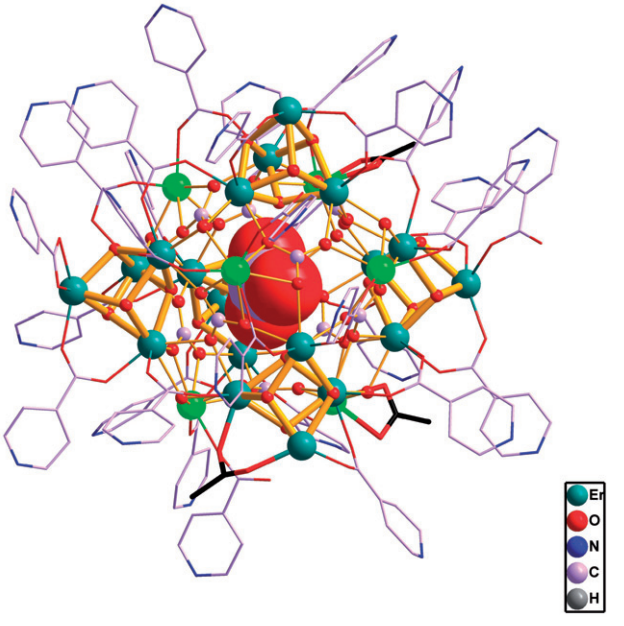


Figure 7. Crystal structure of $Er_{26}$ compound. For clarity, hydrogen atoms and water molecule are omitted and the carbons in $CH_3COO^-$ are increased to black.

### 3.3. *Thermal analysis*

Thermal analyses (figure S3a) of **1** from 35°C to 900°C shows weight loss in several steps. Weight loss of 3.40% from 35°C to 250°C corresponds to the loss of lattice $H_2O$ (Calcd 3.72%). From 250°C to 300°C, weight loss of 3.43% can be attributed to the removal of coordinated $H_2O$ (Calcd 3.35%). As the temperature reaches 300°C, IN ligands are removed and the framework collapses.

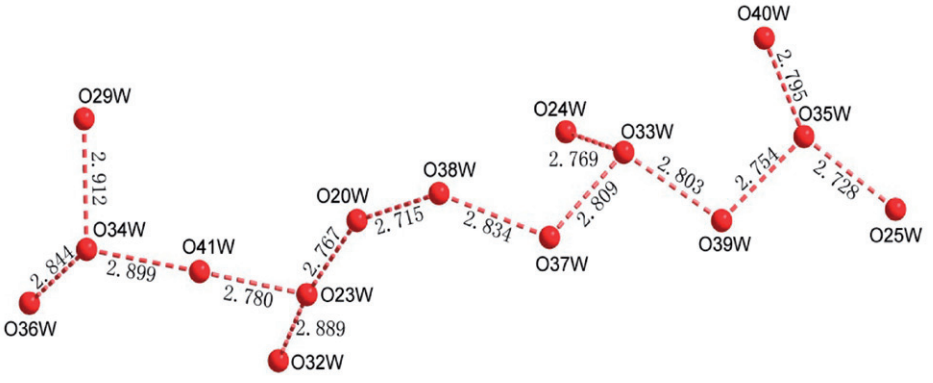


Figure 8. The $(H_2O)_{15}$ water cluster in **2**.

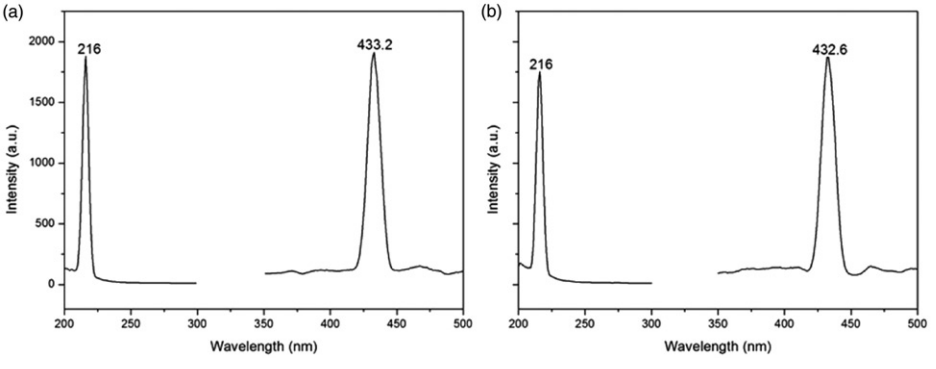


Figure 9. Excitation and emission spectra of **1** (a) and **2** (b).

The TG curve of **2** (figure S3b) from 35°C to 900°C is quite similar to that of **1**. From 35°C to 135°C, loss of 4.63% is attributed to removal of free $H_2O$ (Calcd 4.72%). The second step loss of 3.80% (Calcd 3.45%) from 135°C to 315°C corresponds to the loss of coordinated $H_2O$. The last loss is from the release of IN and the framework collapses over 315°C.

### 3.4. *Optical properties*

Figure 9(a) depicts the excitation and emission spectra of pure **1** in the solid state at room temperature. Blue fluorescence for **1** can be observed, where the maximum emission wavelength is 432.6 nm. The peak with maximum excited light can be observed in excitation spectra at *ca* 216 nm, which is attributed to coordinated HIN; free HIN displays a very weak emission at 431 nm, corresponding to excited light at 330 nm. The fluorescence efficiency of **1** is attributed to the coordination of IN to Ho(III) and strong hydrogen bonding interactions, which effectively increase the rigidity of the ligand reducing the loss of energy by thermal vibrations.

The spectrum of **2** was measured under the same conditions as **1** (as shown in figure 9(b)). While the maximum excited light is also 216 nm, the maximum emission of **2** is at 433.2 nm, a little stronger than **1**, because there is one more $IN^-$ and connections of Er–IN in **2** than in **1**.

## 4. Conclusions

We have prepared two new nanosized clusters built from $CO_3@Ln_{26}$ under hydrothermal conditions. Since the N of $IN^-$ does not coordinate, the two compounds keep discrete structures. In both compounds, four $CO_3@Ln_{26}$ clusters lead to a building unit of $[CO_3@Ln_{26}]_4$ by using $N\cdots Ow$ (water) hydrogen bonding. While adjacent $[CO_3@Ln_{26}]_4$ units are then connected by hydrogen bonds to generate a $[CO_3@Ln_{26}]_{4n}$ layer further bridged by hydrogen interactions to make a 3-D supermolecular framework. The formation of **1** and **2** indicates that replacing a part of bigger ligands by smaller ones can reduce the steric restriction of nanosized cluster and make new solid materials.

## Supplementary material

CCDC-853867 and 853866 contain the supplementary crystallographic data for **1** and **2**. These data can be obtained free of charge *via* http://www.ccdc.cam.ac.uk/conts/retrieving.html, or from the Cambridge Crystallographic Data Centre, 12 Union Road, Cambridge CB2 1E2, UK; Fax: (+44) 1223-336-033; or Email: deposit@ccdc.cam.ac.uk.

## Acknowledgments

We thank the National Natural Science Foundation of China (20971068) for financial support.

## References

[1] M.W. Cooke, G.S. Hanan. *Chem. Soc. Rev.*, **36**, 1466 (2007).
[2] B. Zhao, P. Cheng, X.Y. Chen, C. Cheng, W. Shi, D.Z. Liao, S.P. Yan. *J. Am. Chem. Soc.*, **126**, 3012 (2004).
[3] R. Sessoli, D. Gatteschi, A. Caneschi, M.A. Novak. *Nature*, **365**, 141 (1993).
[4] D. Gatteschi. *Adv. Mater.*, **6**, 635 (1994).
[5] D.E. Katsoulis. *Chem. Rev.*, **98**, 359 (1998).
[6] D. Gatteschi, A. Caneschi, R. Sessoli, A. Cornia. *Chem. Soc. Rev.*, **25**, 101 (1996).
[7] C. Qin, E.B. Wang, Z.M. Su, Y.G. Li, L. Xu. *Angew. Chem. Int. Ed.*, **45**, 7411 (2006).
[8] A. Müller. *Nature*, **397**, 48 (199).
[9] A. Müller, C. Serain. *Acc. Chem. Res.*, **33**, 2 (2000).
[10] A. Müller, E. Beckmann, H. Bögge, M. Schmidtmann. *Angew. Chem. Int. Ed.*, **41**, 1162 (2002).

[11] A. Müller. *Science*, **300**, 749 (2003).
[12] D. Fenske, C. Persau, S. Dehnen, C.E. Anson. *Angew. Chem. Int. Ed.*, **43**, 305 (2004).
[13] D. Fenske, C.E. Anson, A. Eichhöfer, O. Fuhr, A. Ingendoh, C. Persau, C. Richert. *Angew. Chem. Int. Ed.*, **44**, 5242 (2005).
[14] A.J. Tasiopoulos, A. Vinslava, W. Wernsdorfer, K.A. Abboud, G. Christou. *Angew. Chem. Int. Ed.*, **43**, 2117 (2004).
[15] D. Fenske, J. Ohmer, J. Hachgenei. *Angew. Chem. Int. Ed. Engl.*, **24**, 993 (1985).
[16] H. Krautscheid, D. Fenske, G. Baum, M. Semmelmann. *Angew. Chem. Int. Ed. Engl.*, **32**, 1303 (1993).
[17] T. Kajiwara, H. Wu, T. Ito, N. Iki, S. Miyano. *Angew. Chem. Int. Ed.*, **43**, 1832 (2004).
[18] M.R. Bürgstein, M.T. Gamer, P.W. Roesky. *J. Am. Chem. Soc.*, **126**, 5213 (2004).
[19] R. Wang, Z. Zheng, T. Jin, R.J. Staples. *Angew. Chem. Int. Ed.*, **38**, 1813 (1999).
[20] B.Q. Ma, D.S. Zhang, S. Gao, T.Z. Jin, C.H. Yan, G.X. Xu. *Angew. Chem. Int. Ed.*, **39**, 3644 (2000).
[21] S. Natarajan, R. Vaidhyanathan. *Angew. Chem. Int. Ed.*, **43**, 1466 (2004).
[22] X.J. Zheng, L.P. Jin, S. Gao. *Inorg. Chem.*, **43**, 1600 (2004).
[23] J.W. Cheng, J. Zhang, S.T. Zheng, M.B. Zhang, G.Y. Yang. *Angew. Chem. Int. Ed.*, **45**, 73 (2006).
[24] J. Xu, K.N. Raymond. *Angew. Chem. Int. Ed.*, **39**, 2745 (2000).
[25] L.G. Westin, M. Kritikos, A. Caneschi. *Chem. Commun.*, 1012 (2003).
[26] O. Poncelet, L.G. Hubert-Pfalzgraf, J.-C. Daran, R. Astier. *J. Chem. Soc., Chem. Commun.*, 1846 (1989).
[27] R. Wang, H.D. Selby, H. Liu, M.D. Carducci, T. Jin, Z. Zheng, J.W. Anthis, R.J. Staples. *Inorg. Chem.*, **41**, 278 (2002).
[28] Z. Zheng. *Chem. Commun.*, 2521 (2001).
[29] M.B. Zhang, J. Zhang, S.T. Zheng, G.Y. Yang. *Angew. Chem. Int. Ed.*, **44**, 1385 (2005).
[30] R. Anwander. *Angew. Chem. Int. Ed.*, **37**, 599 (1998).
[31] X. Kong, Y. Ren, L. Long, Z. Zheng, R. Huang, L. Zheng. *J. Am. Chem. Soc.*, **129**, 7016 (2007).
[32] X. Kong, Y. Wu, L. Long, L. Zheng, Z. Zheng. *J. Am. Chem. Soc.*, **131**, 6918 (2009).
[33] X.J. Gu, D.F. Xue. *Inorg. Chem.*, **46**, 3212 (2007).
[34] L. Huang, L.J. Han, W.J. Feng, L. Zheng, Z.B. Zhang, Y. Xu, Q. Chen, D.R. Zhu, S.Y. Niu. *Cryst. Growth Des.*, **10**, 2548 (2010).
[35] X.M. Zhang. *Coord. Chem. Rev.*, **249**, 1201 (2005).
[36] G.M. Sheldrick. *SHELXTL (Version 5.10)*, Bruker AXS Inc., Madison, Wisconson, USA (1997).
[37] F. Lloret. *Inorg. Chem.*, **35**, 7384 (1996).
[38] X.J. Gu, D.F. Xue. *Inorg. Chim. Acta*, **361**, 3873 (2008).
[39] M.L. Wei, C.Y. Duan, Q.J. Meng. *J. Am. Chem. Soc.*, **128**, 13318 (2006).
[40] C.Y. Duan, D. Guo, Q.J. Meng. *J. Am. Chem. Soc.*, **132**, 3321 (2010).
[41] M. Hu, J.Y. Yao, H.Q. Su. *J. Coord. Chem.*, **63**, 1744 (2010).
[42] Q.H. Meng, T.R. Qiu, Y.F. Luo. *J. Coord. Chem.*, **63**, 3165 (2010).
[43] W.Y. Yin, Y.S. Ma, R.X. Yuan. *J. Coord. Chem.*, **63**, 1157 (2010).